ESTIMATION OF LINEAR ELECTRICAL MOTOR PERFORMANCE USING FINITE ELEMENT METHOD

Miroslav Bugeza[1], Rastko Fišer[2]

[1]ELEK Svetovanje d.o.o. Ljubljana, Slovenia
[2]University of Ljubljana, Faculty of Electrical Engineering, Slovenia

Key words: linear induction motor, linear synchronous motor, permanent magnet, magnetic field, finite element method, mathematical modeling, propulsion force, attraction force, high-dynamic drive.

Abstract: The paper presents the approach to estimation of operational characteristics of linear induction motor and permanent magnet linear synchronous motor using finite element method. A detailed insight into magnetic field distribution and produced output force is a basic step for motor performance evaluation. A 2D non-linear magnetostatic and eddy-current solver were used for magnetic field and force calculations. The obtained force vectors were decoupled into the propulsion and the attraction force components. The former is vital for determination of motor steady-state and transient characteristics, while the latter is important in mechanical designing of the drive base.

For both types of linear motor calculations were carried out at several excitation currents and different air-gap lengths to optimize the drive performance. The results obtained from the magnetic field calculations could also be applied for determination of motor parameters (e.g. inductances), which are necessary in drive control system simulations. Several laboratory tests were performed to verify the results of the presented method.

Vrednotenje obratovalnih lastnosti linearnih električnih motorjev s pomočjo metode končnih elementov

Ključne besede: linearni asinhronski motor, linearni sinhronski motor, trajni magneti, magnetno polje, metoda končnih elementov, matematično modeliranje, potisna sila, privlačna sila, visoko dinamični pogon.

Izvleček: Članek obravnava postopek določitve obratovalnih karakteristik dveh posebnih tipov električnih motorjev - linearnega asinhronskega motorja in linearnega sinhronskega motorja s trajnimi magneti, ki temelji na uporabi metode končnih elementov. Le-ta omogoča natančen izračun porazdelitve magnetnega polja in vrednosti elektromagnetnih sil, kar je ključnega pomena za zanesljivo oceno pogonskih lastnosti. Glede na različen fizikalni princip delovanja obeh obravnavanih motorjev smo modelirali spremenljivo magnetno polje oziroma uporabili nelinearni magnetostatični izračun. Vektor elektromagnetne sile vsebuje potisno komponento, ki določa zmogljivost pogona ter pritezno komponento, ki jo moramo upoštevati pri dimenzioniranju mehanske konstrukcije pogona.

Za obe vrsti linearnih motorjev so prikazani rezultati izračunov v obliki odvisnosti elektromagnetnih sil od obratovalnih pogojev pri različnih vzbujalnih tokovih in za različne širine zračne reže med gibljivim primarjem in nepremičnim sekundarjem. Iz znanega magnetnega polja je možno določiti še vrsto dodatnih parametrov linearnih motorjev (npr. induktivnosti), ki so pomembni pri modeliranju, simulacijah ali optimiranju nadzorno krmilnega sistema pogona. Realizirani laboratorijski testni pogon dolžine 4 m omogoča meritve električnih in mehanskih parametrov obeh vrst motorjev. Pri doseženi hitrost 2.5 m/s in pospešku 12 m/s^2 je ponovljiva natančnost pozicioniranja 10 μm.

1. Introduction

A machinery construction applying linear electrical motors offers many challenges for engineers and brings up a new philosophy of machine design. In the case of rotational electrical motors it is often required to transform rotation into linear movement, which is unnecessary when using linear motors. The main advantage of linear over the usual rotational motors is outstanding accuracy at high dynamics due to the absence of intermediate gears, screws and crank shafts for linear moving loads. Linear drives are recently used in machine and textile tools, linear tables, saws, shears, separators, transportation systems and many others /1/. As an example, a manufacturer of CNC universal lathes introduced the highly dynamic linear drive (velocity of 100 m/min and acceleration values up to 15 m/s^2), which reduces idle times to a minimum and increases productivity up to 30% by utilization of the latest linear drive technology /2/. At the same time the quality of products increased considerably due to maximum positioning accuracy and precision, which is generally in the contradiction to top-rate dynamics. In addition the contactfree power transfer is almost wear-free, which has a positive effect on the reliability of the machine and reduces maintenance costs.

2. Test drive with linear electrical motors

In *Laboratory of electrical drives* the linear drive was realized as a model of a flying shear, which is a common industrial application for cutting continuous product to a set length. The cutting tools moving in the perpendicular direction are typically mounted on a carriage that moves parallel to the product flow. As it presents linear motion,

usage of the linear motor is preferable /3/. The high cutting speed and the accuracy are major demands for industrial flying shears. The speed depends mainly on the drive dynamic capability and the corresponding construction. Applying the linear motor instead of two rotational ones reduces moving masses thus dynamic performance of the device is higher at the same or even better accuracy of positioning.

Fig. 1 shows the test linear drive, which has the overall length of 4 m. Essential built-in components like linear guideways, bearings, and position sensor guarantee the moving trolley velocity of 2.5 m/s at the acceleration up to 12 m/s^2. The accuracy of the repeated positioning is limited to 10 mm. For achieving even better dynamic and accuracy performance capabilities more sophisticated and expensive components should be selected.

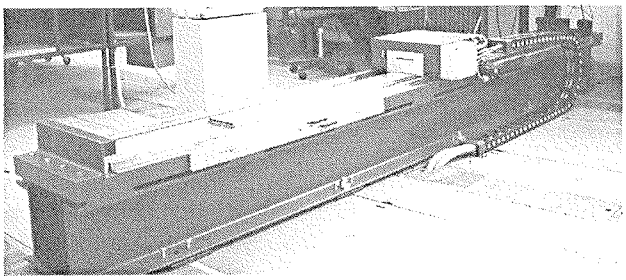

Fig. 1. Test drive with linear electrical motor

The base of linear drive (Fig. 2) was designed for optional application of two linear motor types, the linear induction motor (LIM) and permanent magnet linear synchronous motor (PMLSM), respectively. Basic parameters for both types of linear motors are stated in Table 1.

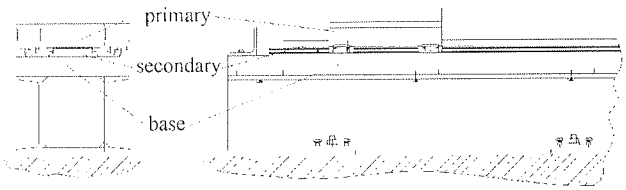

Fig. 2. Main components of the linear drive: base with main plate, primary and secondary part of linear electrical motor

Table 1. Basic constructional and nominal parameters of the linear motors

	Number of pole-pairs	Length of primary (mm)	Length of secondary (mm)	Rated force (N)	Rated current (A)	Rated speed (m/s)
LIM	2	390	3000	1000	19	1
PMLSM	4	390	3000	1500	17	2.5

Both primary parts are relatively similar with slightly distinction in laminations and winding distribution. The main difference is in secondary parts of linear motors. The LIM has the squirrel cage secondary with copper as a conductive material (Fig. 3.a). For induction motors of this size the aluminium squirrel cage would be more common, but since linear motors are not yet manufactured in mass-production such technology is more convenient. Copper bars have also better conductivity, which enables the higher secondary induced currents and improved performance characteristics of the LIM /4/.

The PMLSM has the secondary part (Fig. 3.b) made of rear earth permanent magnets (NdFeB) mounted on soft magnetic backplate, which represents secondary yoke. Permanent magnets are contributing to high magnetic field densities, and consequently to very high energy density of the PMLSM type of linear motor /5/.

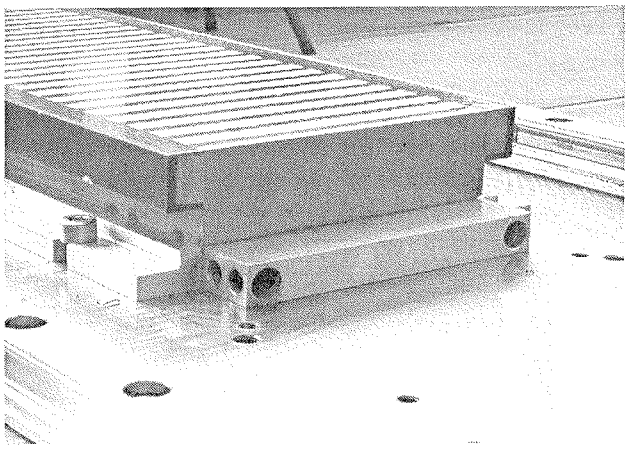

(a)

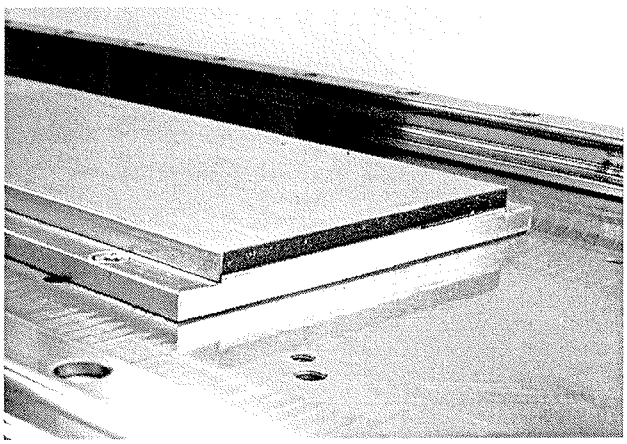

(b)

Fig. 3. Squirrel cage secondary of LIM (a), and PMLSM's secondary part with NdFeB magnets (b)

Although a 4 m drive base plate is relatively long, the final length of the linear drive disables steady-state operation of linear motors. During transients between acceleration and braking, measurements of electrical and mechanical parameters are difficult to perform. Nevertheless for optimal operation of the drive the detailed insight into linear motor performance characteristics is very important /4/, /5/, /

6/. To simulate the steady-state force components characteristics of the LIM and the PMLSM, computation of magnetic field distribution was performed using finite element method (FEM).

3. FEM analyses of linear motor performance

In order to perform a 2D FEM calculations of magnetic field, the motor cross-section was divided into triangular finite elements. To ensure the accurate calculation results the mesh with 16962 triangle elements was generated in the case of LIM (Fig. 4.a), and 13772 triangle elements in the case of PMLSM (Fig. 4.b), respectively. In order to reduce the complexity of the geometry and the number of nodes of finite element mesh, the calculations are usually performed over the smallest symmetrical part of the rotational motor model. This simplification cannot be applied in the case of linear motors due to the asymmetrical magnetic field distribution and longitudinal end-effects /6/. In Fig. 5 the details of finite element mesh in one magnetic pole of the LIM and PMLSM are shown.

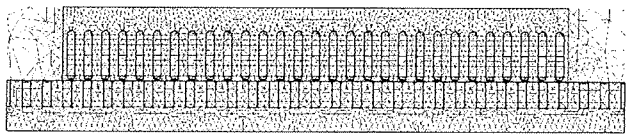

(a)

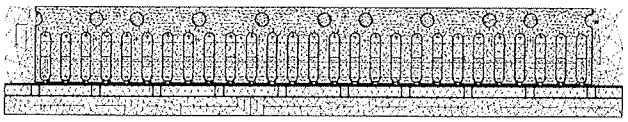

(b)

Fig. 4. Finite element mesh in the cross-section of LIM (a), and PMLSM (b)

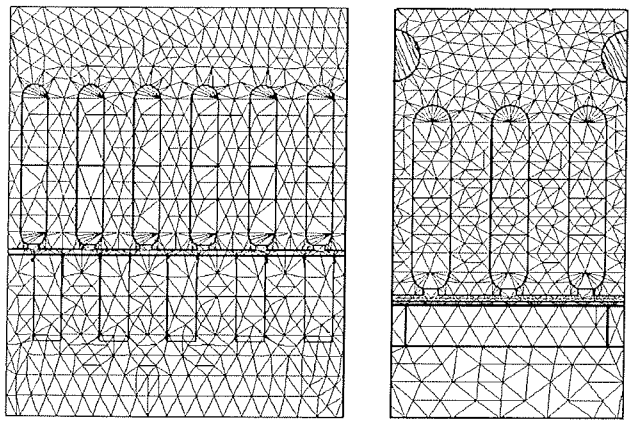

(a) (b)

Fig. 5. Finite element mesh in detail of one magnetic pole of LIM (a), and PMLSM (b)

3.1. FEM calculation of LIM magnetic field

When the velocity of the moving primary part differs from the velocity of the longitudinal traveling magnetic field, eddy-currents of the slip frequency are induced in the squirrel cage of the LIM's secondary part. In such case the magnetic field is described with Helmholtz differential equation

$$\vec{\nabla}\times(\frac{1}{\mu}\cdot\vec{\nabla}\times\vec{A})=\sigma\cdot\vec{\nabla}\phi-\sigma\cdot\frac{\partial\vec{A}}{\partial t} \qquad (1)$$

where m is permeability, $\vec{A}$ is magnetic vector potential, s is conductivity and f is electric scalar potential. Magnetic vector potential $\vec{A}$ is calculated by the implementation of a 2D eddy-current solver.

Due to 2D field calculation, which disables the secondary loops configuration, the secondary cage was modelled as passive conductors that means they have eddy and displacement currents flowing through them, but have no component of source current. All secondary conductors (bars) are defined to be connected parallel in short circuit, which in fact represents two end-rings /7/. In this procedure variations of material properties and excitations can be considered. Except in the case of locked secondary condition, the currents and flux density in secondary and primary part are pulsating at different frequencies. Since the computation is done using phasor analysis, all calculated variables must be of the same frequency. To resolve this difficulty we can define primary excitation currents as ampere-turns with frequency corresponding to instantaneous slip value by parametric calculation for chosen steady-state points. Such approach enables simulation of running conditions at many secondary speed values from start-up to no-load condition using very simple and unexpensive FEM software.

3.2. FEM calculation of PMLSM magnetic field

In the case of PMLSM type of linear motor, the primary part velocity is synchronized with longitudinal magnetic field, and the magnetic field is described with the Poisson differential equation

$$\vec{\nabla}\times(\frac{1}{\mu}\cdot\vec{\nabla}\times\vec{A})=\vec{J} \qquad (2)$$

where $\vec{J}$ represents the current density, which consists of excitation currents in primary three-phase winding and equivalent magnetizing current of permanent magnets / 8/, /9/.

Permanent magnets used in PMLSM secondary part are NdFeB - Vacodim 633. The equivalent magnetizing current used in FEM model was determined from demagnetizing characteristics shown in Fig. 6.

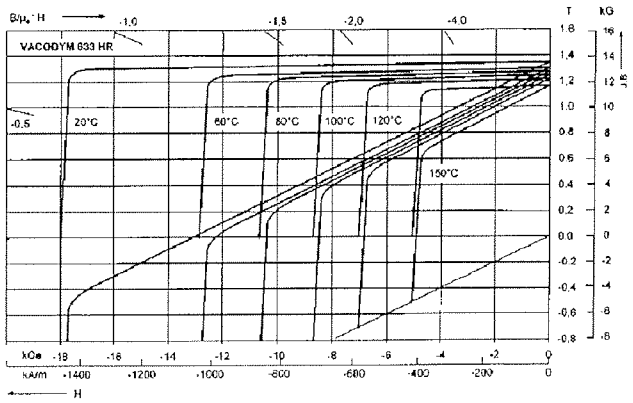

Fig. 6. Demagnetizing characteristics of Vacodym 633

For mechanical protection of permanent magnets the protective plate made of stainless steel is applied (Fig. 3b). At steady-state the velocity of the PMLSM equals to the synchronous speed, thus the conductive protective plate has no influence on propulsion force. Contrary at transient states, induced currents in the protective plate contribute the additional component to the propulsion force thus reduces oscillations, while the velocity of the moving primary increases or decreases /10/. To estimate this phenomenon the eddy-current solver was used like in the case of LIM type of linear motor. The comparison of the calculated total propulsion force and components due to the induced currents in the protective plate shows that the influence of induced currents in the protective damper plate can be neglected, especially at higher loads /11/.

3.3. Magnetic field distribution

The primary parts of both types of linear motors have a two-layer winding with half-filled end slots, which is typical topology /1/. Because of this constructional particularity the number of poles is odd. Contrary to the magnetic field in rotational motors, which is always symmetrically distributed along the air-gap, the magnetic conditions in linear motors are regularly asymmetrical.

Fig. 7a shows the magnetic field distribution of LIM at maximal force at slip 0.12. The same case of maximal force for PMLSM at maximal load angle 90° is presented in Fig. 7b. The boreholes of the water-cooling system are placed in the yoke of the PMLSM primary lamination (Fig. 7b). They obviously have an additional effect on asymmetrical magnetic flux distribution. The LIM also has a water-cooling system, however aluminium units are mounted above the primary and under the secondary parts and have no influence on the flux lines. The magnetic field distribution in a detail of one magnetic pole of the LIM and PMLSM are presented in Fig. 8a and Fig. 8b, respectively.

The magnetic field in the LIM is excited by currents in primary winding. Due to the half-filled end slots winding the magnetic field distribution in the air-gap is unproportional regarding magnetic pole division (Fig. 9.a). In the PMLSM the magnetic field is excited by currents in primary winding

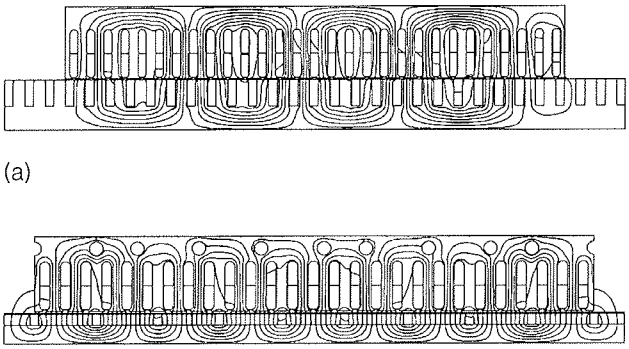

(a)

(b)

Fig. 7. Magnetic field distribution in the cross-section of LIM (a), and PMLSM (b)

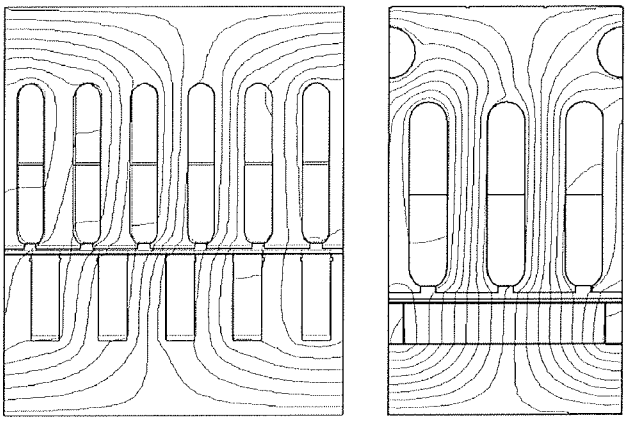

(a) (b)

Fig. 8. Magnetic field distribution in a detail of one magnetic pole of LIM (a), and PMLSM (b)

and NdFeB permanent magnets, thus the PMLSM's air-gap field distribution is more proportional (Fig. 9b).

The NdFeB permanent magnets used in PMLSM are capable of producing strong magnetic field, therefore the average air-gap flux density is much higher (0.91 T) in comparison to the LIM's average air-gap flux density (0.49 T), which represents a 54 % difference in benefit of the PMLSM. This distinction between both described types of linear motors is obvious also from the nominal data presented in Table 1. For the same physical size and similar primary excitation currents is the nominal propulsion force of the LIM 1000 N, while for the PMLSM is denoted to 1500 N. Such higher power density of the PMLSM in comparison to the LIM is the main reason, that the PMLSM type of linear motor is much more often used in machine tool applications. Nevertheless for more robust, less dynamic and cheaper applications (e.g. longer transportation tracks) the choice of the LIM type of linear motor would be more appropriate solution.

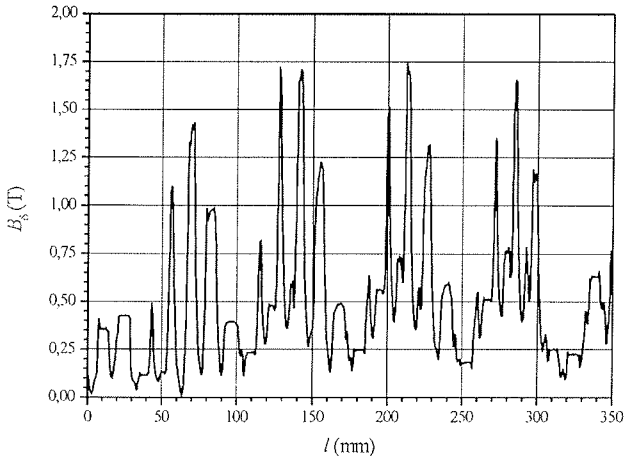

(a)

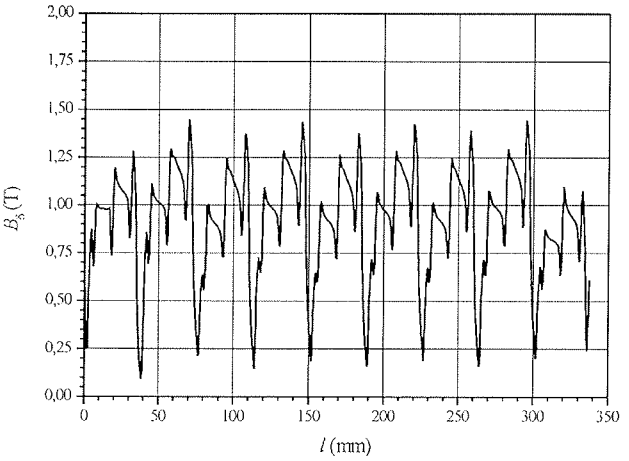

(b)

Fig. 9. Air-gap magnetic flux density distribution of LIM (a), and PMLSM (b)

4. Simulation of steady-state force characteristics

The electromagnetic force of the LIM was calculated from magnetic field results by Maxwell's stress tensor. The differential equation for the force $\vec{F}$ produced on a surface is:

$$d\vec{F} = \frac{1}{2}(\vec{H}\cdot(\vec{B}\cdot\vec{n}) + \vec{B}\cdot(\vec{H}\cdot\vec{n}) + (\vec{H}\cdot\vec{B})\cdot\vec{n}) \qquad (3)$$

where $\vec{H}$ is magnetic field intensity, $\vec{B}$ is magnetic flux density and $\vec{n}$ is normal vector on the surface. When force components for the whole range of movement are computed, the steady-state force characteristic can be determined. The calculated force vector consists of propulsion force F_x and attraction force F_y. The propulsion force determines the performance characteristics of the linear motor, while the attraction force between primary and secondary part is in fact parasitic and thus it has to be taken into account when designing the construction of the drive set-up.

For both motors the propulsion force characteristics were calculated at different excitation currents. Fig. 10a shows steady-state force characteristics of the LIM and Fig. 10b the ones of the PMLSM. There is obvious influence of detent force in PMLSM characteristics, which could be reduced in a design phase with an appropriate choice of secondary configuration and permanent magnet length / 12/. As expected approximately two times higher excitation primary current is reqired in the LIM to achieve the same propulsion force as in the case of the PMLSM.

Characteristics of the attractive force between primary and secondary part are shown in Fig. 11. At the same excitation primary current the ratio of attractive to maximal propulsion force is about 5 in case of the LIM and 4.2 in the case of the PMLSM.

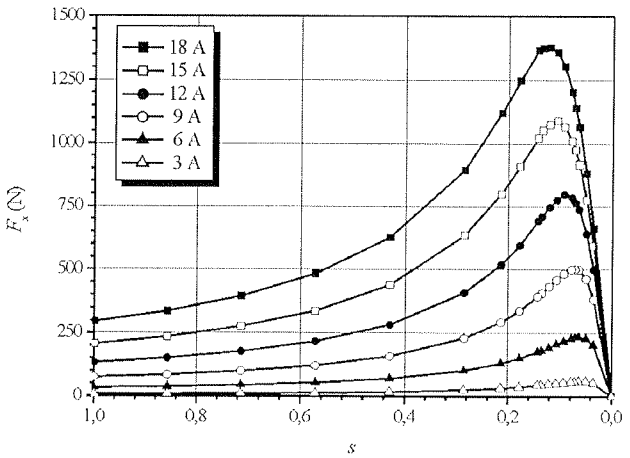

(a)

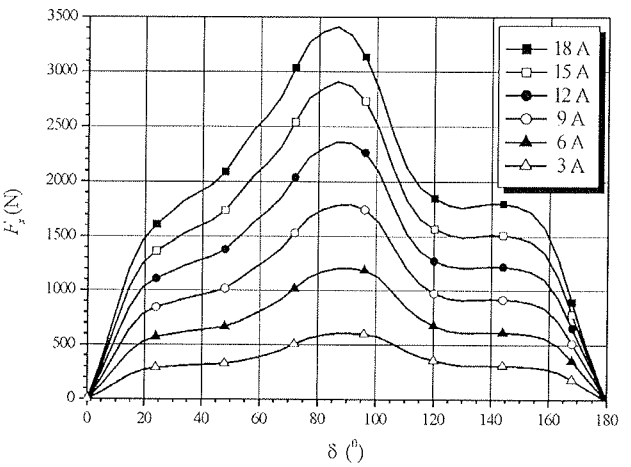

(b)

Fig. 10. Propulsion force characteristics at different excitation currents of LIM (a), and PMLSM (b)

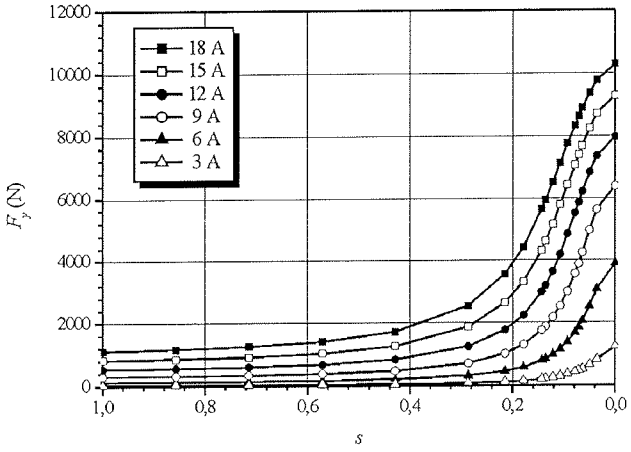

(a)

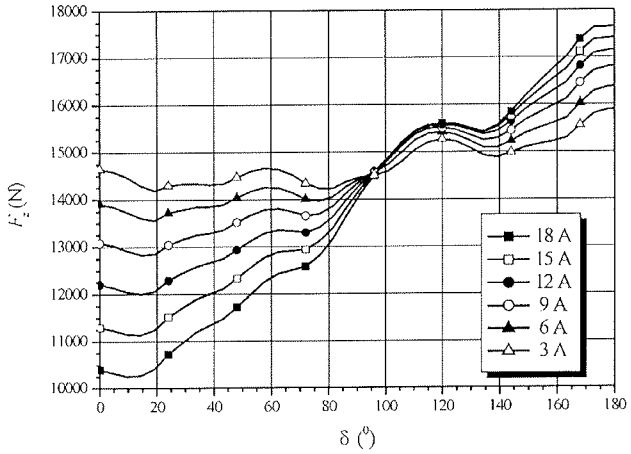

(b)

Fig. 11. Attraction force characteristics at different excitation currents of LIM (a), and PMLSM (b)

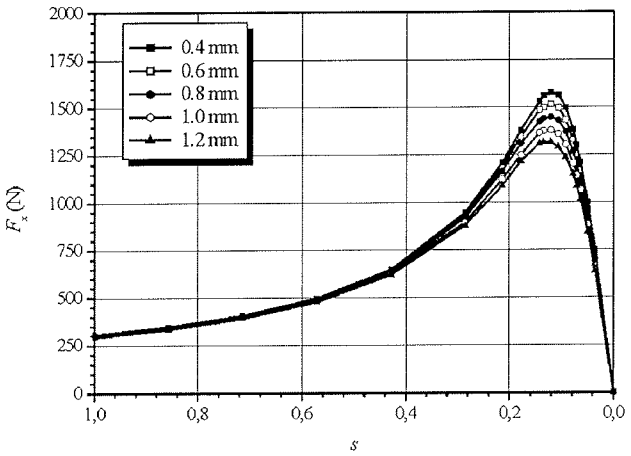

(a)

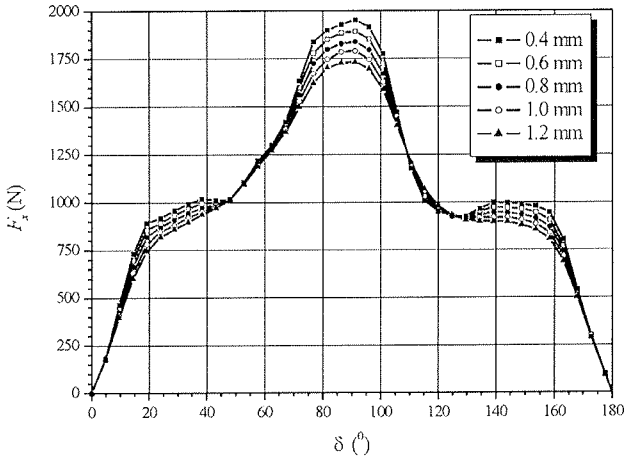

(b)

Fig. 12. Propulsion force characteristics for different air-gap lengths of LIM (a), and PMLSM (b)

The PMLSM produces the same propulsion force at just half of the current of the LIM. For adequate comparison the force characteristics for different air-gap lengths have to be calculated at different excitation currents: for example 18 A for the LIM and 9 A for the PMLSM. Comparison of such characteristics is presented in Fig. 12. While the air-gap was changing from 0.4 mm to 1.2 mm, the propulsion force declined for 18.8 % in the case of LIM and for 12.8 % in the case of PMLSM.

5. Experimental results

Since the geometry and material properties can be fully taken into account, the magnetic field results also enable precise determination of several others variable motor parameters (e.g. inductances), which are used in further research of LIM's and PMLSM's operational performance. For study of transient operation, which is in fact the case when dealing with limited drive lenght of linear motors, nonlinear dynamic simulation models were developed. Detailed explanations of such models are reported in /13/ for the LIM and in /14/ for the case of PMLSM.

During research several measurements were performed on laboratory models of the LIM and the PMLSM. Fig. 13a shows transient velocity response (start-up, steady-state, reversing, stand-still), while Fig.13b presents propulsion force of the LIM at several increasing load levels. The active load of the test drive is connected to the primary of the linear motor via a steel cable. Oscillations occur due to the strain of the steel cable. The same test for the PMLSM type of motor is shown in Fig. 14. Both motors are supplied and controlled by the same inverter thus demonstrate similar results although it can be noticed that PMLSM has smoother performance due to more rigid force characteristic.

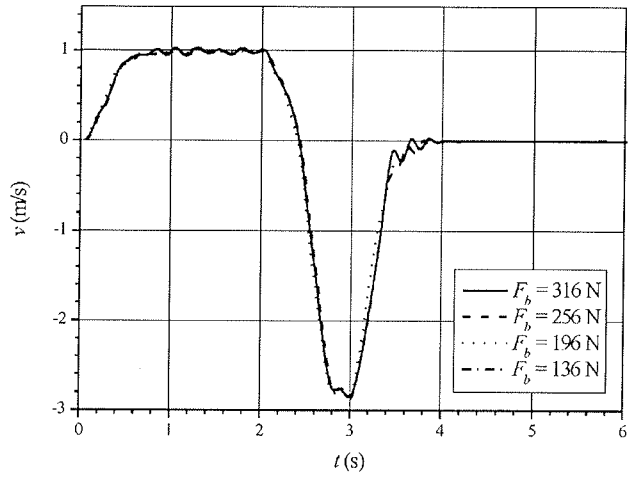

(a)

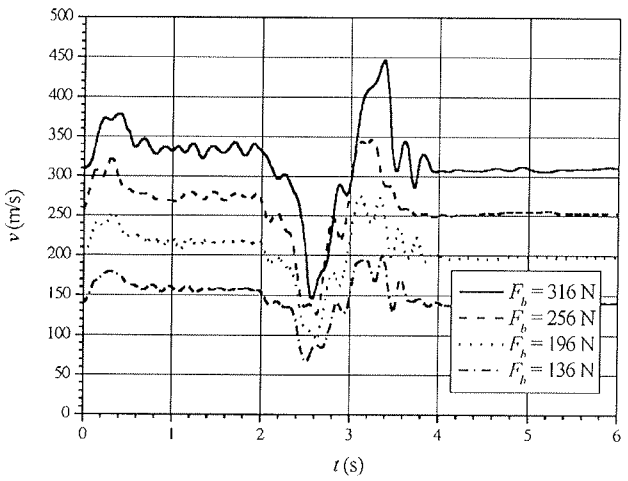

(b)

Fig. 13. Measured velocity and propulsion force transients of LIM at increasing load

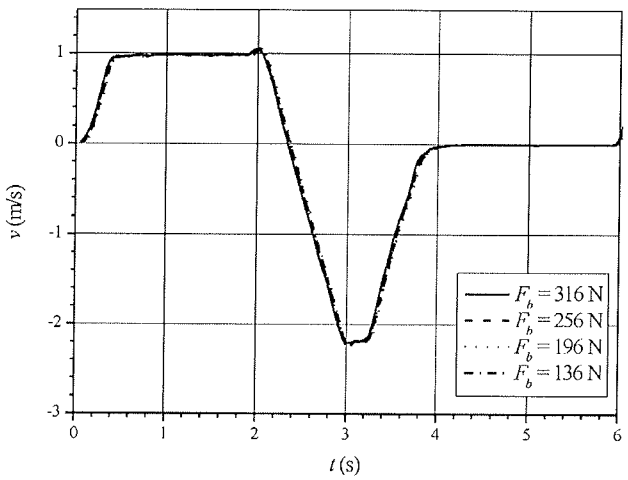

(a)

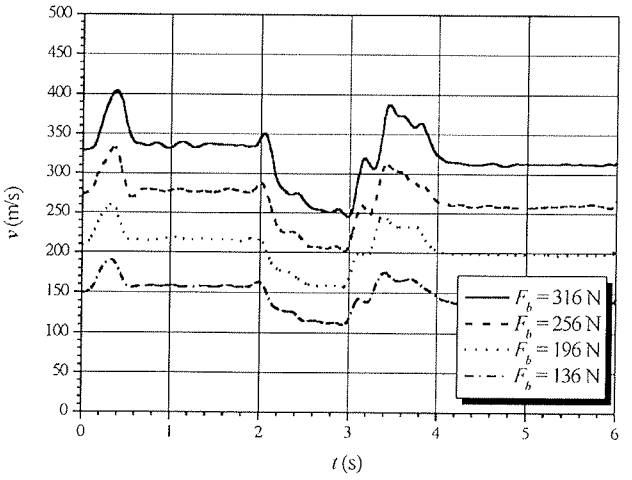

(b)

Fig. 14. Measured velocity and propulsion force transients of PMLSM at increasing load

6. Conclusions

Both types of linear motors are designed to achieve the best possible performance characteristics - LIM's squirrel cage made of copper, and NdFeB permanent magnets in the PMLSM' secondary part. Intense electrical and mechanical transients cause difficulties during measurements of motor parameters, therefore FEM magnetic field computations are of great importance for detailed insight into the motors operational characteristics.

From force calculation results it is obvious, that the PMLSM has higher propulsion force at the same excitation currents, furthermore the ratio between the attraction and the propulsion force components is lower than in the case of the LIM. As expected, the overall comparison of the LIM and the PMLSM type of linear motors reveals, that the PMLSM has better performance characteristics for high-dynamic applications. Employing permanent magnets in motor design, the dimensions of the PMLSM are smaller, thus more appropriate for servo drives. Nevertheless the LIM still has the advantage, when lower price or simpler and more robust construction are required.

7. References

/1/ I. Boldea, S.A. Nasar, *Linear Motion Electromagnetic Devices*, Taylor&Francis, 2001.

/2/ www.gildemeister.com.

/3/ S. Ceferin, M. Bugeza, R. Fišer, "Linear Synchronous Drive in flying Shear Application", *Electromotion Journal*, Vol. 12,No. 2/3, pp. 161-165, 2005.

/4/ J.F. Gieras, *Linear Induction Drives*, Oxford, Claredon Press, 1994.

/5/ J.F. Gieras, *Linear Synchronous Motor: Transportation and Automation Systems*, London, CRC Press, 2000.

/6/ M. Poloujadoff, *The Teory of Linear Induction Machinery*, Oxford, Claredon Press, 1980.

/7/ R. Fišer, S. Ferkolj, "Application of a Finite Element Method to Predict Damaged Induction Motor Performance", *IEEE Transaction on Magnetics*, Vol. 37, No. 5, September 2001, pp. 3635-3639.

/8/ C. M. Ong, *Dynamic Simulation of Electrical Machinery*, Prentice Hall, New Jersey, 1998.

/9/ M. Bugeza, D. Makuc, R. Fišer, "Estimation of Nonlinear Equivalent Circuit Elements Using Finite Element Method", EPNC 2004, Poznań, Poland, June 28-30, 2004, *Conference Proceedings*, pp. 37-38.

/10/ D. Miljavec, "Finite Element Method in Evaluation of Torque Ripple in Synchronous Reluctance Motor", *Compel*, Vol. 17, Nr. 1/2/3, 1998, pp. 369-373.

/11/ M. Bugeza, R. Fišer, "Estimation o Permanent Magnet Protective Plate Effect on Dynamic Characteristics of PMLSM", *Przeglad Electrotechniczny*, Nr. 5, 2006, pp. 26-29.

/12/ S.M. Jang, S.H. Lee, I.K. Yoon, "Design Criteria for Detent Force Reduction of Permanent-Magnet Linear Synchronous Motors With Halbach Array", *IEEE Transactions on Magnetics*, Vol. 38, No. 5, September 2002.

/13/ M. Bugeza, R. Fišer, "Dynamic model of linear induction motor", ISEF 2005, Baiona, Spain, September 15-17, 2005, *Conference Proceedings*, pp. 1-5.

/14/ M. Bugeza, D. Makuc, R. Fišer, "Dynamic model of permanent magnet linear synchronous motor", ICEM 2004, Cracow, Poland, September 5-8, 2004, *Conference proceedings*, pp. 1-6.

Asst. Miroslav Bugeza, M.Sc.
ELEK svetovanje d.o.o. Ljubljana
Marice Kovačeve 7, SI - 1000 Ljubljana, Slovenia
Phone: +386 (0)1 5654 050; Fax: +386 (0)1 5654 055
E-mail: miro@elek.si

Asst. Prof. Dr. Rastko Fišer, univ. dipl. ing.
University of Ljubljana, Faculty of Electrical Engineering
Tržaška 25, SI - 1000 Ljubljana, Slovenia
Phone: +386 (0)1 4768 280; Fax: +386 (0)1 4264 630
E-mail: rastof@fe.uni-lj.si

Prispelo (Arrived): 08.11.2006 *Sprejeto (Accepted):* 30.03.2007